NACA

RESEARCH MEMORANDUM

BOUNDARY-LAYER MEASUREMENTS ON SEVERAL POROUS

MATERIALS WITH SUCTION APPLIED

By George B. McCullough and Bruno J. Gambucci

Ames Aeronautical Laboratory
Moffett Field, Calif.

NATIONAL ADVISORY COMMITTEE
FOR AERONAUTICS

WASHINGTON

NATIONAL ADVISORY COMMITTEE FOR AERONAUTICS

RESEARCH MEMORANDUM

BOUNDARY-LAYER MEASUREMENTS ON SEVERAL POROUS

MATERIALS WITH SUCTION APPLIED

By George B. McCullough and Bruno J. Gambucci

SUMMARY

Boundary-layer velocity profiles were measured on ten samples of various porous materials and on an impervious aluminum plate mounted flush with the inner surface of the side wall of a small wind tunnel. Suction was applied to the back side of the porous test materials through a 4-inch-square opening. The profiles were measured after the natural boundary layer of the tunnel wall had traversed a distance of 3-1/2 inches along the suction area.

The boundary layer measured on the smooth impervious plate was laminar at the upstream end of the suction area, but was of the transitional type after having traversed the 3-1/2 inches to the downstream measuring station. Without suction none of the velocity profiles measured on the porous materials were laminar at the downstream station. The thickness of the boundary layer was increased and its form altered from that measured on the impervious plate by amounts which depended on the nature of the surface of the material. With suction applied the form of the boundary layers was greatly altered, and both the displacement thickness and the momentum thickness were reduced. The rate of thinning diminished with increasing suction, and the boundary-layer displacement and momentum thicknesses on all of the porous materials appeared to be approaching a low ultimate value with increasing suction velocity.

INTRODUCTION

A method of boundary-layer control based on the continuous removal of a portion of the boundary-layer flow along a porous surface has been the subject of several recent investigations. This method has been termed "distributed" or "area suction" to distinguish it from suction through discrete slots cut in an otherwise impervious surface, and has received particular attention because theoretical analyses indicate that

it is more economical of power than the method employing slots. Area
suction may be used for three general purposes: to increase the maximum
lift of a wing by delaying separation of either the laminar boundary
layer near the leading edge or the turbulent boundary layer near the
trailing edge; to reduce drag by delaying transition of the boundary-
layer flow to turbulence; or to improve the efficiency of inlets or
diffusers by thinning the boundary-layer flow (references 1, 2, and 3).

The investigation reported herein was made in connection with an
investigation of area suction intended to delay separation of the laminar
boundary layer near the leading edge of an airfoil section. It was the
the purpose of the present investigation to gain in a quick and simple
manner some idea of the importance of the nature of the surface of vari-
ous porous materials on the boundary layer flowing over the materials.
Precise and detailed measurements which would provide a check on the
theory of boundary-layer flow with porous suction were not made, nor were
measurements made of the pressure differential or power required to
induce the suction flow. It was felt, however, that the information
obtained would serve as a rough guide for the selection of porous mate-
rials where it was desired to maintain the thinnest possible boundary
layer with the minimum volume of suction flow.

The tests were made in a small wind tunnel and consisted of
measurements of the boundary-layer velocity profiles on small samples of
various porous materials inset into the side walls of the wind tunnel.
Measurements were made for several ratios of the average suction velocity
to free-stream velocity from 0 to 0.0182. In addition, measurements were
made on a smooth, impervious aluminum plate to serve as a basis for
assessing the effects of the roughness of the porous materials.

NOTATION

A nominal area to which suction was applied, 0.111 square feet

g acceleration of gravity, 32.2 feet per second squared

h local total pressure within boundary layer, pounds per square foot

H settling-chamber total pressure, pounds per square foot

p_0 reference static pressure measured at entrance to test section,
      pounds per square foot

p local static pressure measured along center line of test-section
      wall, pounds per square foot

u   local velocity within boundary layer $\left(\sqrt{\dfrac{2}{\rho_o}(h-p)}\right)$, feet per second

U_1 local velocity outside of boundary layer, feet per second

U_o free-stream velocity $\left(\sqrt{\dfrac{2}{\rho_o}(H-p_o)}\right)$, feet per second

v_s average suction velocity $\left(\dfrac{W_a}{g\rho_o A}\right)$, feet per second

y   distance from surface, inches

$R_\delta *$ boundary-layer Reynolds number $\left(\dfrac{U_1 \delta *}{\nu}\right)$

R_θ boundary-layer Reynolds number $\left(\dfrac{U_1 \theta}{\nu}\right)$

W_a weight rate of suction flow, pounds per second

δ boundary-layer thickness, inches

$\delta *$ boundary-layer displacement thickness $\left[\displaystyle\int_o^\delta \left(1-\dfrac{u}{U_1}\right)dy\right]$, inches

θ boundary-layer momentum thickness $\left[\displaystyle\int_o^\delta \dfrac{u}{U_1}\left(1-\dfrac{u}{U_1}\right)dy\right]$, inches

ν kinematic viscosity, feet squared per second

ρ_o free-stream density, slugs per cubic foot

MATERIALS AND APPARATUS

Materials

Ten samples of four different types of porous materials were
investigated. All of the materials are commercially available as flat
sheets. The samples were 4-5/8 inches square, and the thickest one did
not exceed 3/32 inch. The various samples are listed in table I together
with remarks about the surface roughness. Photographs of the samples,
both direct and with a magnification factor of 21, are presented in
figure 1.

One of the materials was a laboratory-type filter paper which
required additional support in the wind tunnel, and hence was tested
with two different backing materials: a 16 mesh, 0.023-inch-diameter wire
screen (sample 1), and a flat, electroplated, 40-count metal mesh
(sample 2).

The second type of material was a woven wire filter cloth with
250 woof (longitudinal) threads and 20 warp (transverse) threads per
inch. This material was tested in two positions; that is, with the woof
parallel with the flow (sample 3), and with the warp parallel with the
flow (sample 4).

The third type of material was a metal mesh with square openings
made by an electroplating process. Two sizes of mesh, 40 count
(sample 5), and 65 count (sample 6), were tested. The percent open area
of the 40-count mesh was 23.0, and of the 65-count mesh was 10.5.

The fourth type of material was sintered bronze of which four
samples of varying porosity were tested. Samples 7, 8, and 9 were
intended for use in filters, and sample 10 was originally impregnated
with oil for use in bearings. The oil was removed for these tests, but
the porosity was so low that only low suction velocities could be
attained with the suction pump.

The degree of surface roughness varied greatly between the various
samples. Because of the nature of the materials it is difficult to
assess the surface roughness from purely geometric considerations. This
is particularly true of the wire cloth and the electroplated mesh. Also
the surfaces of the samples of sintered bronze are not analogous to the
surface of a smooth flat plate on which small granules of some sandlike
material have been sprinkled in such a manner that each grain can be
considered as an individual roughness element. Measurements were made,
however, with the aid of an instrument which drew greatly magnified pro-
files of the surface of the filter paper and the sintered bronzes. These
profiles were difficult to interpret in terms of roughness because the

datum or "surface" from which the height of the roughness elements were
to be measured was not clear. Instead, the average total amplitude of
each set of curves was taken as a measure of the surface roughness. The
sintered bearing material (sample 10) felt as smooth to the touch as
the aluminum plate on which the basic boundary-layer velocity profiles
were obtained. All the other samples felt rougher in varying degrees.

Wind Tunnel

     The small wind tunnel used in the investigation is of the nonreturn
type and has a closed, rectangular throat. The tunnel is powered by a
variable-speed electric motor which drives an aircraft-type centrifugal
compressor (supercharger). The air is pumped into a settling chamber
where it passes through four fine-mesh wire screens before entering the
contraction cone. From the contraction cone the air flows through a
rectangular test section and is exhausted to the atmosphere through a
diffuser. The dimensions of the throat are 2.1 by 7.4 inches. The floor
and ceiling (2.1-inch dimension) of the test section diverge a total
of 1.0° in the vertical plane to compensate partially for boundary-layer
growth. The contraction ratio of the tunnel is 15.5 to 1. The turbu-
lence level is unknown.

Auxiliary Equipment

     The 4-5/8-inch-square test samples were mounted in a recess over a
4-inch-square opening symmetrical with the center line of the test-
section side wall. The porous materials, therefore, overlapped the
suction area by 5/16 inch on all four sides. The upstream edge of the
suction area was 3/8 inch downstream of the beginning of the test section.
A photograph of a test sample mounted in the wind tunnel is shown in
figure 2.

     A plenum chamber was fastened to the outside of the tunnel wall and
was connected by a duct containing an orfice-type flow meter to an
annular ejector pump. This pump was operated by compressed air, the flow
of which was manually regulated to produce the desired suction velocity
through the porous material. The ejector pump exhausted into the dif-
fuser of the wind tunnel. A diagram of the arrangement is shown in
figure 3.

     The boundary-layer velocity profiles were measured with a single
total-pressure tube. The shank of the tube was bent at right angles and
projected through a tight-fitting hole in the side of the tunnel. The
height of the tube above the surface could thus be changed from outside

the tunnel. The distance of the tube above the surface was read on an
Ames dial gage. The surface was defined as the level indicated by the
dial gage with the tip of the probe just touching the porous surface.
In some cases the point of first contact was verified with the tunnel
running by measuring the electrical resistance between the probe and the
porous metal. The tip section of the probe was made of 0.015-inch-
diameter, 0.0025-inch-wall-thickness tubing flattened to 0.010 inch.
The geometric center of the tube was taken as the effective center. The
distance above the surface corresponding to each determination of the
local velocity within the boundary layer, therefore, was taken as the
net reading of the dial gage plus 0.005 inch. In most cases the effec-
tive or aerodynamic surface of the porous material was undoubtedly below
the nominal surface by an amount which depended on the heights of the
roughness elements, but because of the previously mentioned uncertainty
in the measurements of surface roughness, no corrections were applied to
take this factor into account. The axis of the probe was in the median
plane of the tunnel with the tip extending 1/2 inch ahead of the down-
stream edge of the suction area. The boundary layer on the tunnel wall
traveled a distance of 3-1/2 inches over the suction area before reach-
ing the measurement station. With the aluminum plate installed in the
tunnel, an additional measurement was made at the upstream boundary of
the suction area. With the porous materials the presence of the plenum
chamber on the outside of the test-section wall made it impractical to
install the probe at this upstream station.

                               TESTS AND RESULTS

     Each test sample was carefully fitted into the test-section wall
and, except for the samples of filter paper, the joints and screw holes
were filled with surfacing putty which was sanded down flush with the
surface. The filter paper was faired in with modeling clay to avoid the
sanding operation.

     The dynamic pressure was held constant at 30 pounds per square foot
which corresponds to a tunnel speed of about 165 feet per second and a
Mach number of 0.143. The Reynolds number per foot of length was
about 1,000,000. For the porous materials, five rates of the average
suction velocity were used: 0, 0.6, 1.0, 2.0, and 3.0 feet per second.

     The distribution of static pressure along the center line of the
side wall of the wind tunnel is shown in figure 4. The boundary-layer
velocity profiles measured on the aluminum plate are shown in figure 5.
The two profiles shown for the downstream station were measured for two
different installations of the plate. Because repeat runs for the same
installation showed good agreement, the difference in the two profiles
can be attributed only to differences in the degree of smoothness of the

joints in the test-section wall. The boundary-layer profiles measured on the porous materials are shown in figure 6. It is possible that these measurements were also affected by the degree of smoothness with which the various samples were fitted into the wall, but any discrepancies in the data from this cause would not be sufficient to alter the general conclusions of this report. Also shown for comparison is the thicker of the two velocity profiles measured at the same station on the aluminum plate.

DISCUSSION

Measurements on the Impervious Plate

In considering the boundary-layer measurements on the impervious plate, there are several factors to be noted which would influence the growth of the boundary layer up to the plate. The boundary-layer flow prior to reaching the test region was subjected to acceleration in the contracting section of the tunnel. The boundary-layer measurements, however, were made in a region of essentially zero pressure gradient (fig. 4). Also, although pains were taken to keep the tunnel wall smooth, the flow may have been subjected to two surface discontinuities, one at the upstream edge of the removable side wall and the other at the upstream edge of the inset test plate.

The velocity profile measured at the upstream end of the plate (fig. 5) was of the laminar type and showed the effect of the acceleration in the contracting section of the tunnel. It was typical of the laminar type in a favorable pressure gradient as shown by comparison with a profile computed by the Pohlhausen approximate method for $\lambda = +12$. (The parameter λ specifies the velocity gradient, and +12 corresponds to the most favorable gradient the method will permit without producing unrealistic profiles. See reference 4.)

At the downstream station a difference in velocity profile was obtained, as previously mentioned, for two different installations of the test plate which was apparently due to differences in the surface condition at the upstream end of the test plate. The two profiles resembled neither laminar nor fully developed turbulent profiles. It is probable that the measurement station was in a region of intermittent transition and, therefore, the measured velocity profiles represent the time average of fluctuating dynamic pressures within the boundary layer.

In an attempt to shed further light on the nature of the boundary layers, the boundary-layer Reynolds number R_θ and R_δ^* were computed using values of the momentum thickness θ and the displacement thickness δ^* obtained by mechanical integration of the velocity profiles.

At the upstream station the respective values were: θ, 0.0045 inch; δ^*, 0.0091 inch; R_θ, 367, and R_δ^*, 745. While the value of R_δ^* is not high for a laminar boundary layer in a zero pressure gradient, it is sufficiently large to indicate that transition could be imminent in a stream with a moderately high level of turbulence. At the downstream station, the thicker of the two profiles gave the following values: θ, 0.0117 inch; δ^*, 0.0186 inch; R_θ, 956, and R_δ^*, 1520. Although the magnitude of R_δ^* is not beyond the realm of possiblity for a laminar boundary layer, the shape of the velocity profile indicates that it is not laminar. If the boundary layer is undergoing transition, as is believed to be the case, then the computed values of the boundary-layer parameters have little meaning because they do not represent a steady-state velocity profile.

Measurements on Porous Materials Without Suction

For zero suction velocity, the porous sample which produced the least effect on the boundary layer was sample 10 (the bearing material). The velocity profile was almost identical with that on the aluminum plate (fig. 6(j)). It was, however, the most dense of all the porous samples and permitted a maximum suction velocity of only 1.0 foot per second with the suction pump used.

Aside from sample 10, the two smoothest samples were the filter paper, which showed little effect of the types of backing (figs. 6(a) and (b)), and the sintered bronze, sample 9 (fig. 6(i)). The velocity profiles for zero suction on both of these materials showed a considerable difference from the velocity profile on the aluminum plate, and are definitely of the turbulent type.

The profiles measured with samples 3 to 8 (figs. 6(c) to 6(h)) showed large effects of surface roughness. The profile which showed the greatest difference from that measured on the aluminum plate was that for sample 5, the coarser of the two electroplated meshes. The orientation of the wire cloth (figs. 6(c) and 6(d)) also had an effect on the boundary layer: a thicker profile resulted with the warp parallel to the flow than with the woof parallel to the flow.

Measurements on Porous Materials With Suction

The effect of suction on the boundary-layer velocity profiles on all of the porous materials was about the same. The velocity near the surface was increased, and the total thickness of the boundary layer was reduced. In order to illustrate further the effect of suction, each velocity profile was integrated and the boundary-layer displacement

thickness δ^*, and the momentum thickness θ ascertained. The values of
these parameters are plotted in figure 7 as functions of the suction
velocity ratio v_s/U_o. The trend is the same for all materials; a rapid
decrease of δ^* and θ with increasing suction velocity ratio.
Both δ^* and θ appear to be approaching small ultimate values for high
suction velocity ratios. From considerations of attaining the thinnest
possible boundary layer with the minimum suction velocity, materials
which are physically smooth with small closely spaced pores such as
samples 8, 9, or 10 are best. Materials with definite open spaces like
the electroplated meshes are poor. For high suction-velocity ratios,
however, the degree of surface roughness appears to be of diminishing
importance as compared to the case for zero suction. If the power
required to produce the suction is taken into consideration, the choice
of materials may be considerably affected because a large power require-
ment may more than counterbalance the apparent advantage offered by a
dense smooth-surfaced material.

In an attempt to shed further light on the nature of the profiles
measured with suction in the present investigation, comparison was made
with the profiles presented in references 3 and 5. These references
report the results of boundary-layer measurements made on a flat, porous
plate with suction, and compare the experimentally derived profiles
with those predicted by theory. Reference 3 is concerned with turbu-
lent flow and reference 5 with laminar flow. Neither the theoretical
nor the experimental laminar suction profiles of reference 5 (which were
in good agreement) are similar to the suction profiles of the present
investigation; hence it may be concluded that the latter are not laminar.
They are, however, similar to the turbulent suction profiles of refer-
ence 5. It is also shown in reference 5 that an asymptotic turbulent
profile, analogous to the asymptotic laminar profile, can be attained
with turbulent flow (i.e., that there will be no further change in the
boundary-layer profile with increasing distance downstream). A method
for computing the shape of the asymptotic turbulent profile is derived
and, according to this analysis, the portion of the profile outside
the laminar sublayer is a function of the logarithm of the distance from
the surface. A simple check on experimental profiles can be obtained by

plotting the values of $\left(1 - \dfrac{u}{U_o}\right)$ against $\log_e y$. For an asymptotic

turbulent profile the outer portion of the boundary layer should be a
straight line. The suction profiles measured in the present investi-
gation were plotted in this manner and did not produce straight lines
even though the suction-velocity ratios were higher than those employed
in reference 3. This would indicate that the length of the suction area
in the present investigation (3-1/2 in.) was not sufficient for the
velocity profile to attain its ultimate form.

CONCLUDING REMARKS

From the measurements of boundary-layer velocity profiles on several porous materials for ratios of suction velocity to free-stream velocity varying from 0 to 0.0182, it was shown that for zero and low values of suction velocity the degree of surface roughness produced a considerable effect on the thickness of the boundary layer; the greater the surface roughness, the thicker the boundary layer. Materials such as the flat metal meshes with definite open spaces, although smooth to the touch, were shown to be aerodynamically rough. In general, increasing the suction velocity reduced the boundary-layer thickness rapidly at first; then, at a rate which diminished with increasing suction. The boundary-layer displacement thickness and momentum thickness for all the porous materials appeared to be approaching a low ultimate value for suction-velocity ratios greater than the maximum attained in these tests.

Ames Aeronautical Laboratory
    National Advisory Committee for Aeronautics
        Moffett Field, Calif.

REFERENCES

1. Thwaites, B.: A Theoretical Discussion of High-Lift Aerofoils with Leading-Edge Porous Suction. R. & M. No. 2242, British A.R.C., 1946.

2. Ulrich, A.: Theoretical Investigation of Drag Reduction in Maintaining the Laminar Boundary Layer by Suction. NACA TM 1121, 1947.

3. Kay, J. M.: Turbulent Boundary Layer Flow with Uniform Suction. British A.R.C. 12,193, 1949.

4. Durand, W. F., ed., Aerodynamic Theory. Vol. III, Julius Springer (Berlin), 1934.

5. Kay, J. M.: Experimental Investigation of Boundary Layer Flow Along a Flat Plate with Uniform Suction. British A.R.C. 11,476, 1948.

TABLE I.- LISTING OF THE SAMPLES TESTED

Sample number	Figure number of photograph	Type of material	Remarks	Measured roughness (in.)
1	1(a)	Filter paper	Backed with wire screen	[a]0.0007
2	1(a)	- - do. - -	Backed with electroplated mesh	[a]0.0007
3	1(b)	Woven wire cloth	Woof parallel with flow	- - -
4	1(b)	- - do. - -	Warp parallel with flow	- - -
5	1(c)	Square mesh made by electroplating	40 count	- - -
6	1(d)	- - do. - -	65 count	- - -
7	1(e)	Sintered bronze	Manufacturers' grade 2	[b]- - -
8	1(f)	- - do. - -	Manufacturers' grade 4	0.005
9	1(g)	- - do. - -	- - - -	0.0025
10	1(h)	- - do. - -	De-oiled bearing material	0.0012

[a]This low measured value is probably misleading because the softness of the paper may have allowed surface fibers to sink into the body of the paper under the pressure of the measuring stylus.

[b]Too rough to measure directly, but average diameter of individual particles appeared to be at least ten times greater than that of grade 4.

Page intentionally left blank
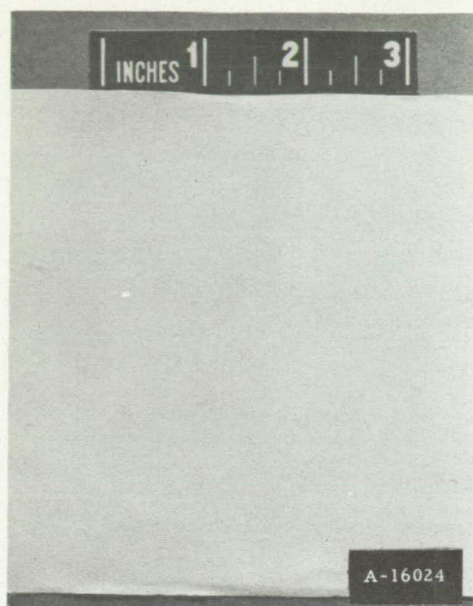
(a) Samples 1 and 2 (filter paper).
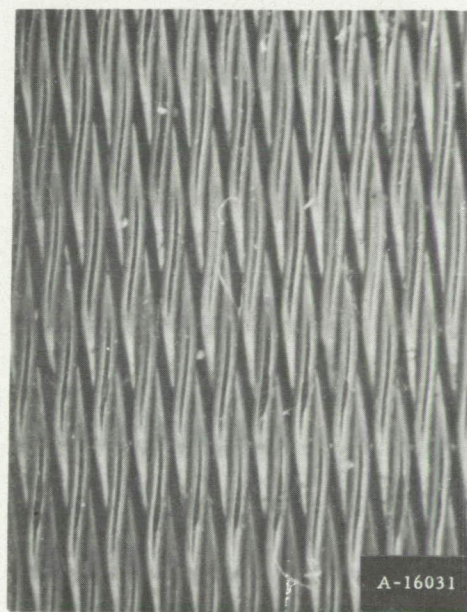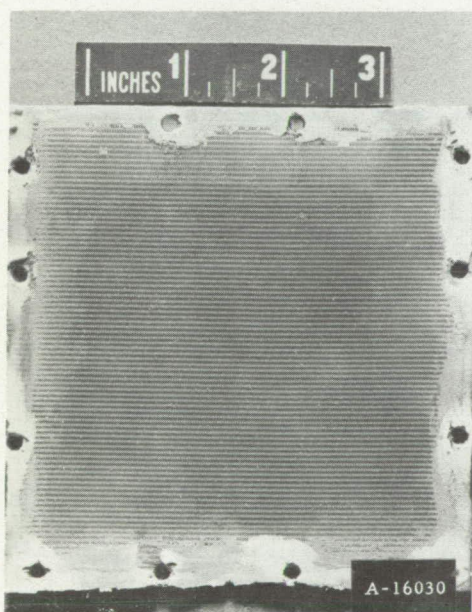
(b) Samples 3 and 4 (wire cloth).

Figure 1.- Photographs of the samples of porous materials. Magnification ratio is 21X.
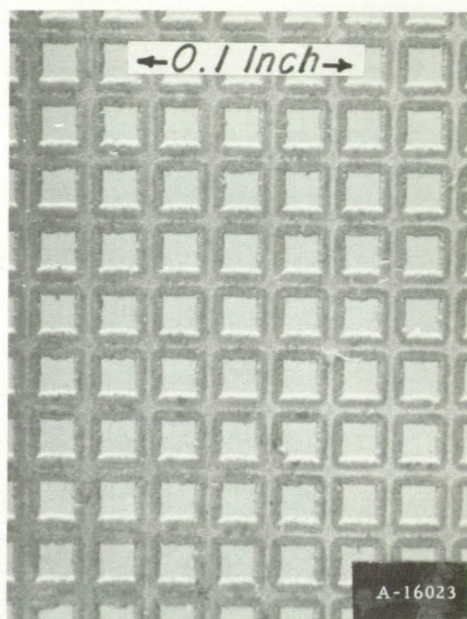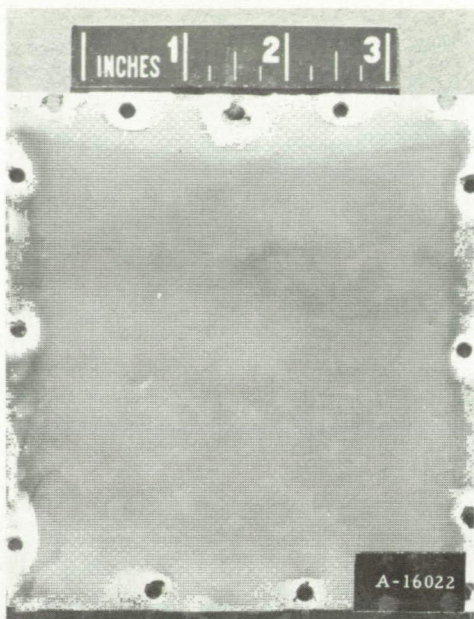
(c) Sample 5 (40-count mesh).
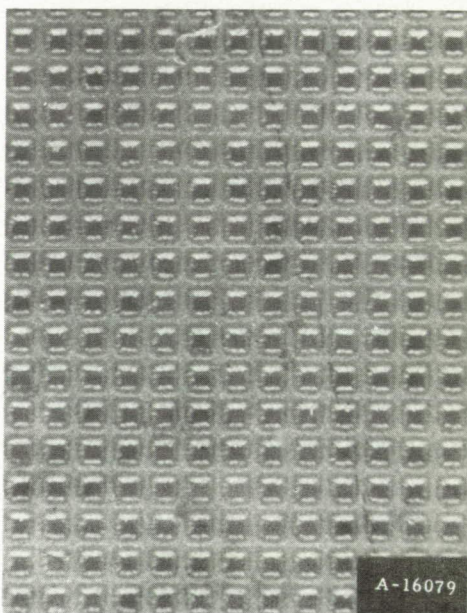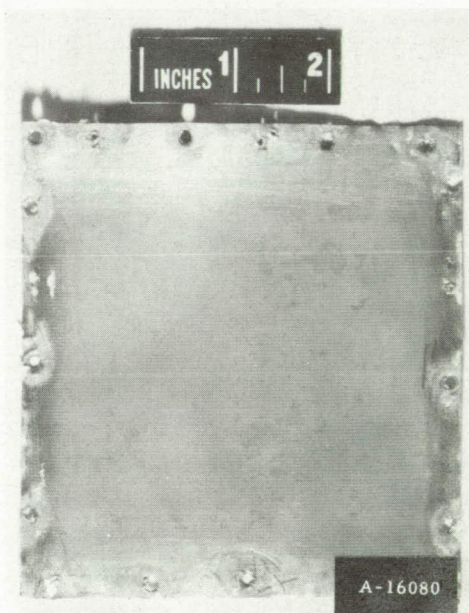
(d) Sample 6 (65-count mesh).

Figure 1.- Continued.
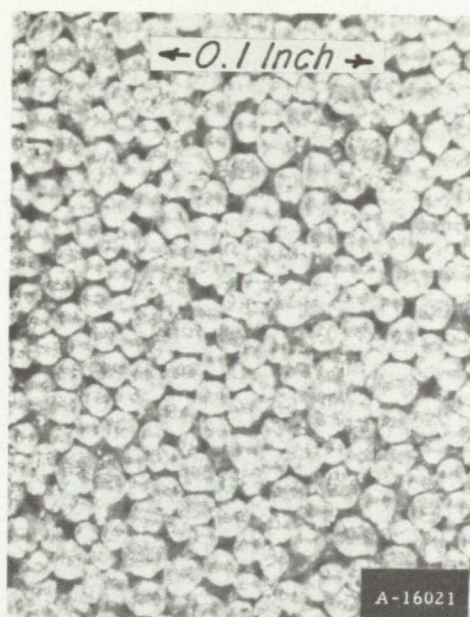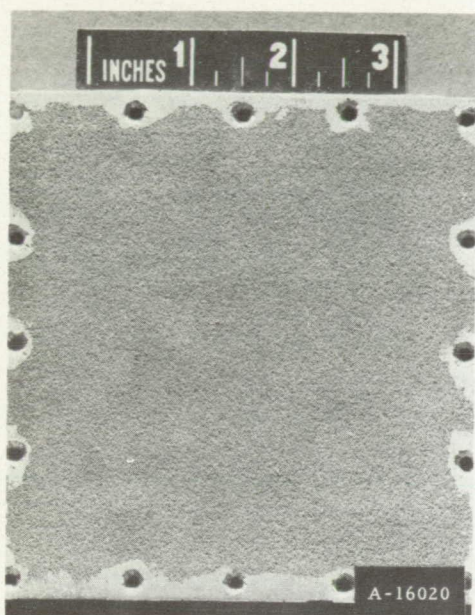
(e) Sample 7 (sintered bronze).
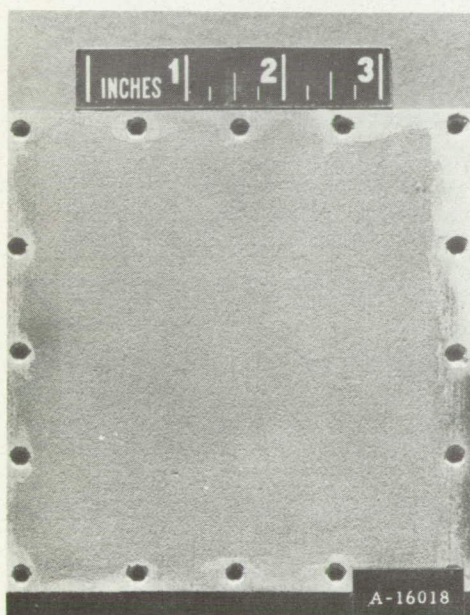
(f) Sample 8 (sintered bronze).
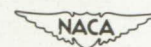
Figure 1.- Continued.
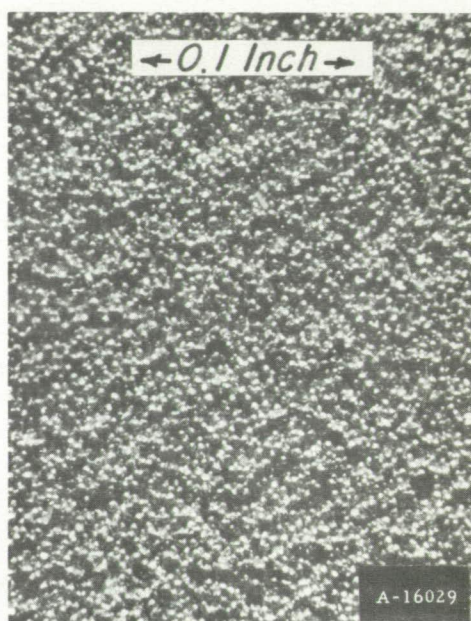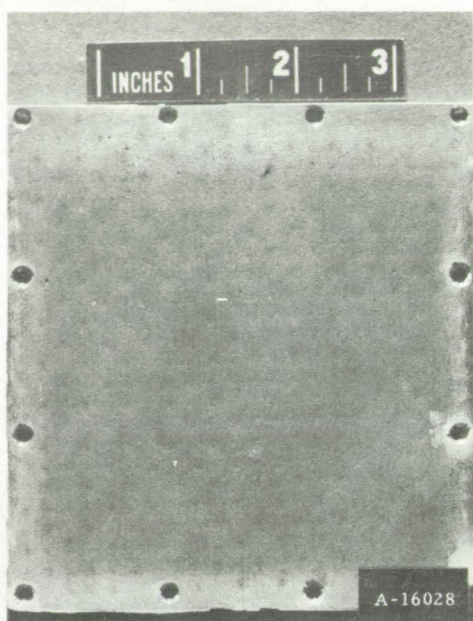
(g) Sample 9 (sintered bronze).
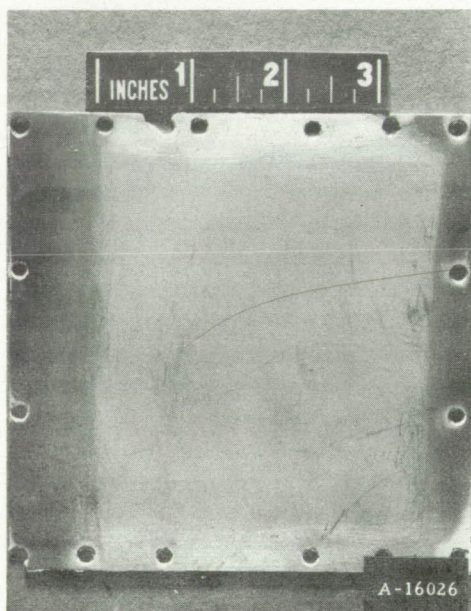
(h) Sample 10 (sintered bronze)

Figure 1.- Concluded.
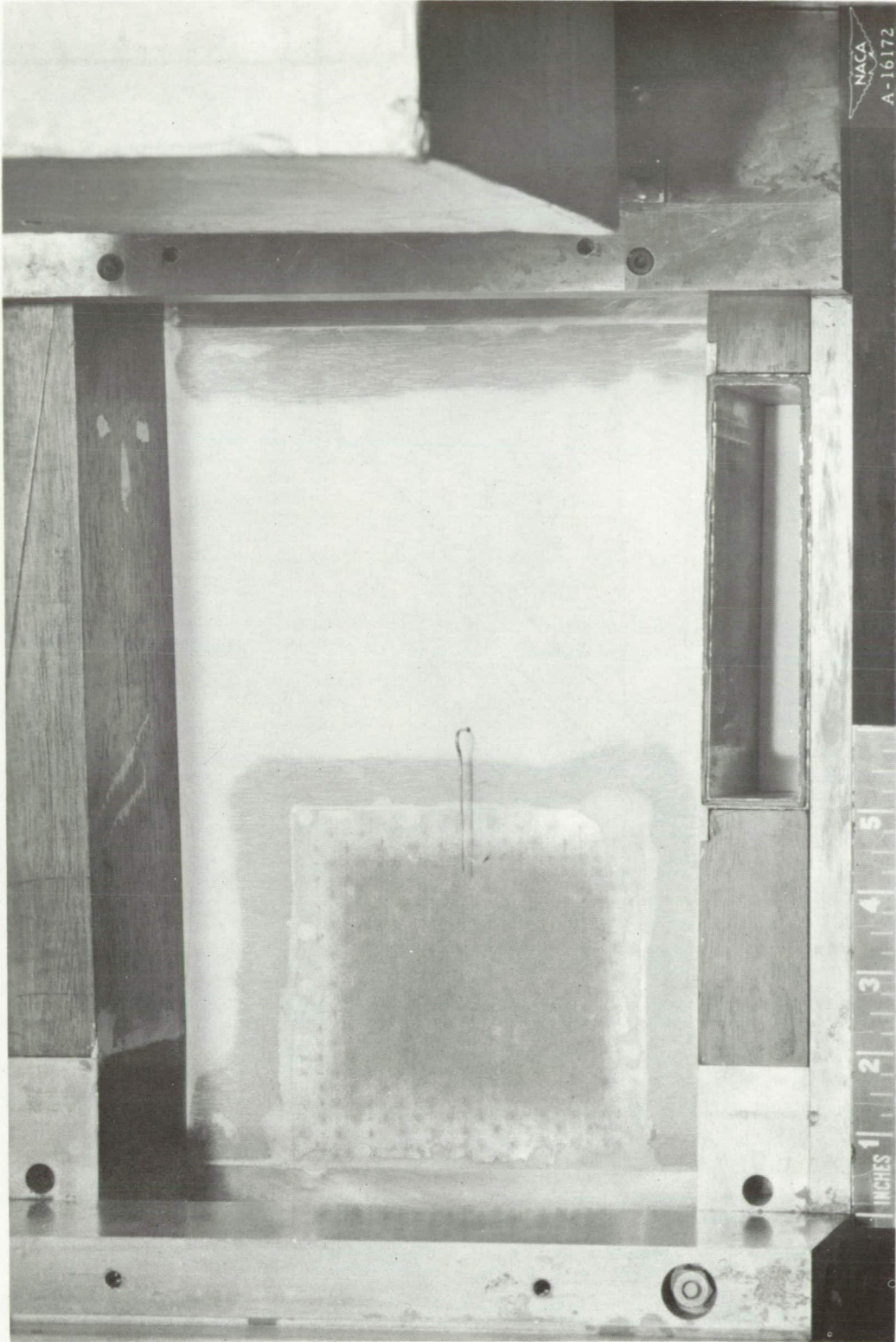
Figure 2.- Test sample mounted in the wind tunnel.

Figure 3.- Diagram of test setup.
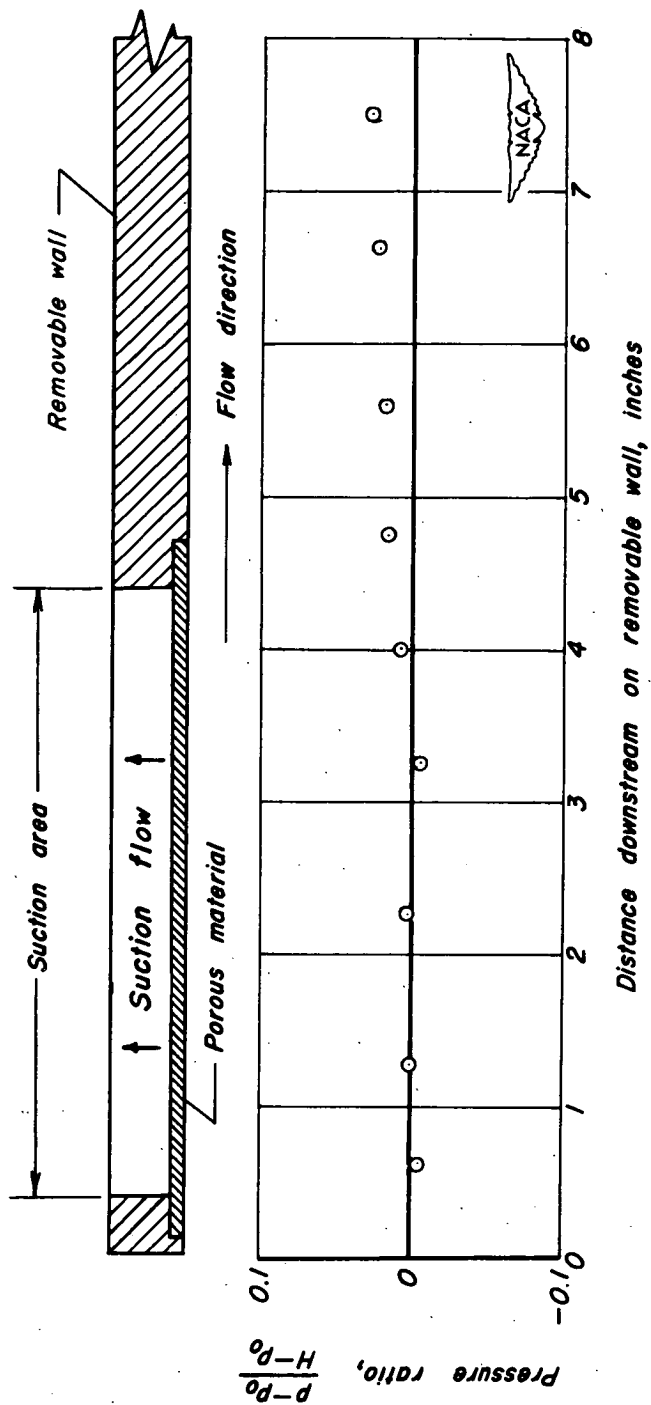
Figure 4.— Pressure distribution along horizontal center line of test—section wall.
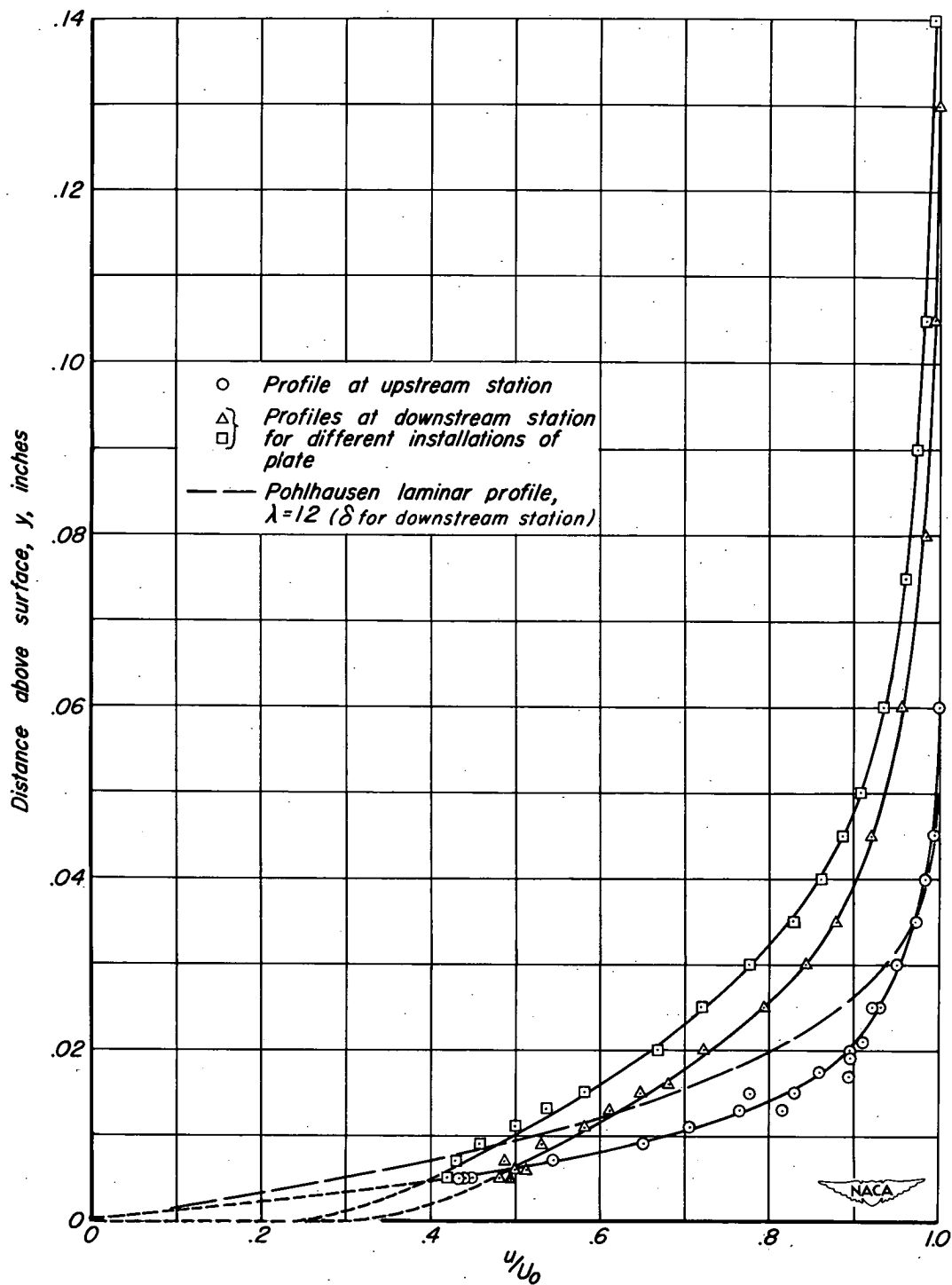
Figure 5.— Boundary-layer velocity profiles on impervious aluminum plate.
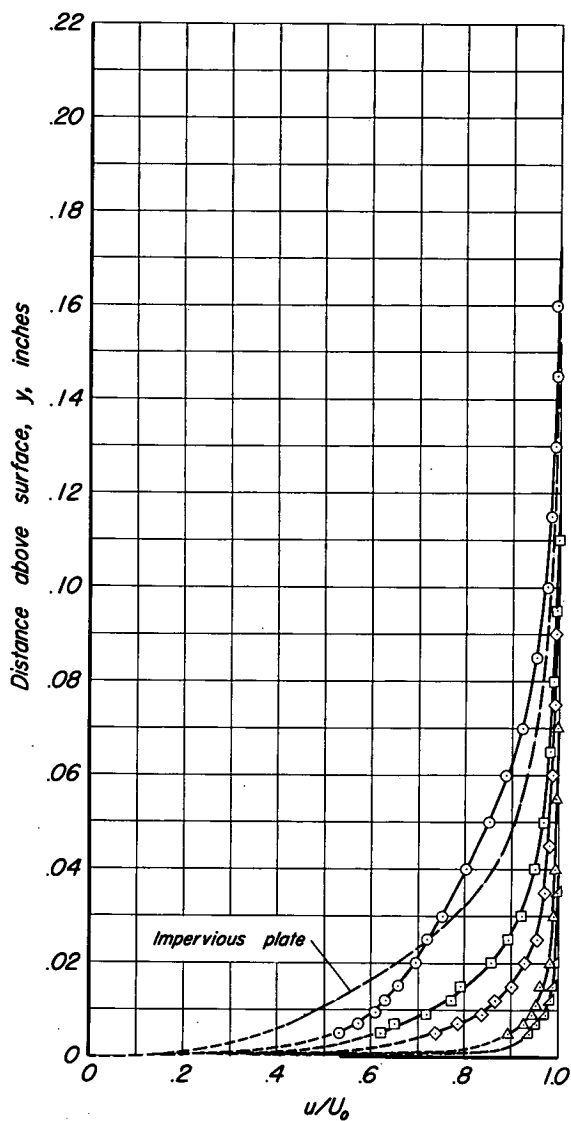
(a) Sample I, (filter paper with wire
    screen backing).
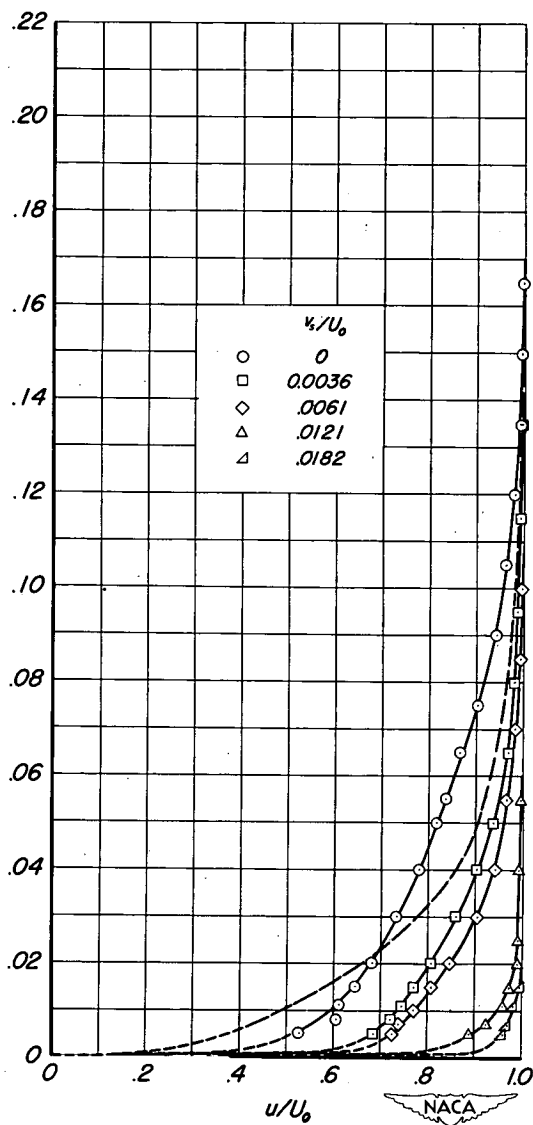
(b) Sample 2, (filter paper with electro-
    plated mesh backing).

Figure 6 .—Boundary-layer velocity profiles on several porous materials
with various suction velocities.
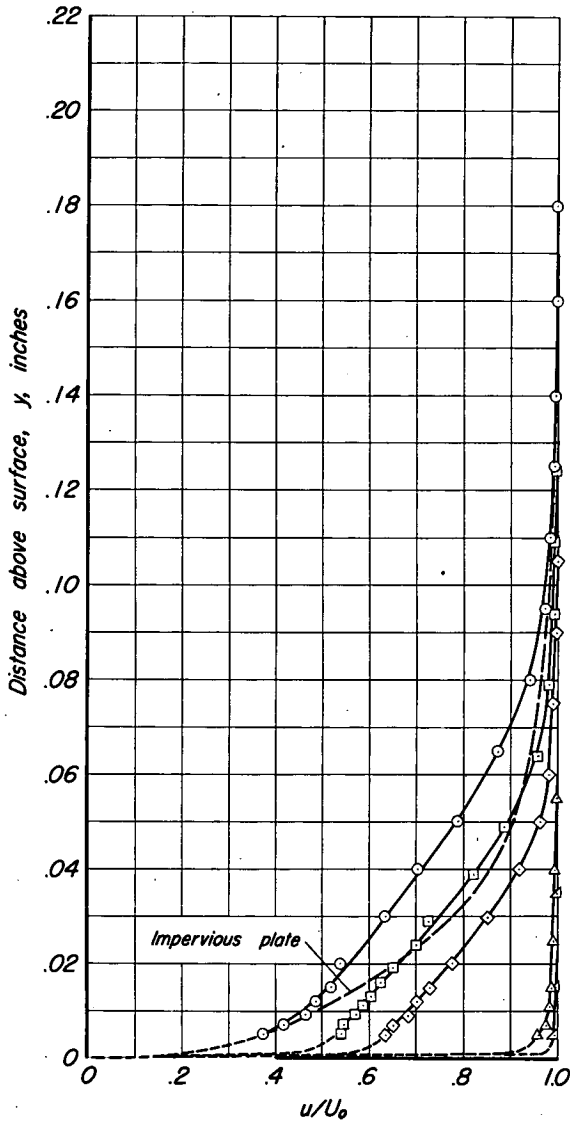
(c) Sample 3, (wire cloth with woof
parallel with flow).
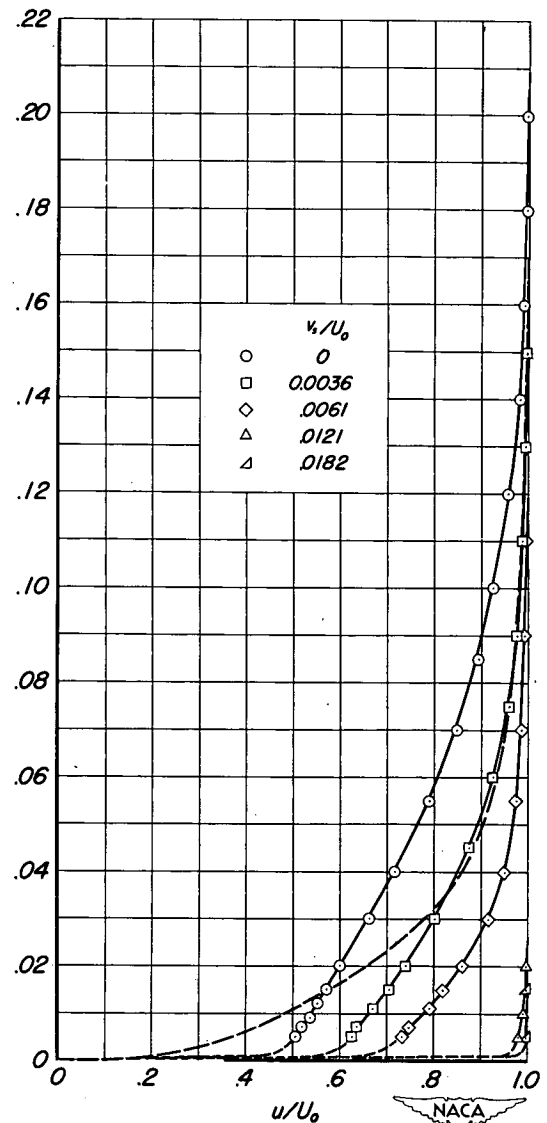
(d) Sample 4, (wire cloth with warp
parallel with flow).
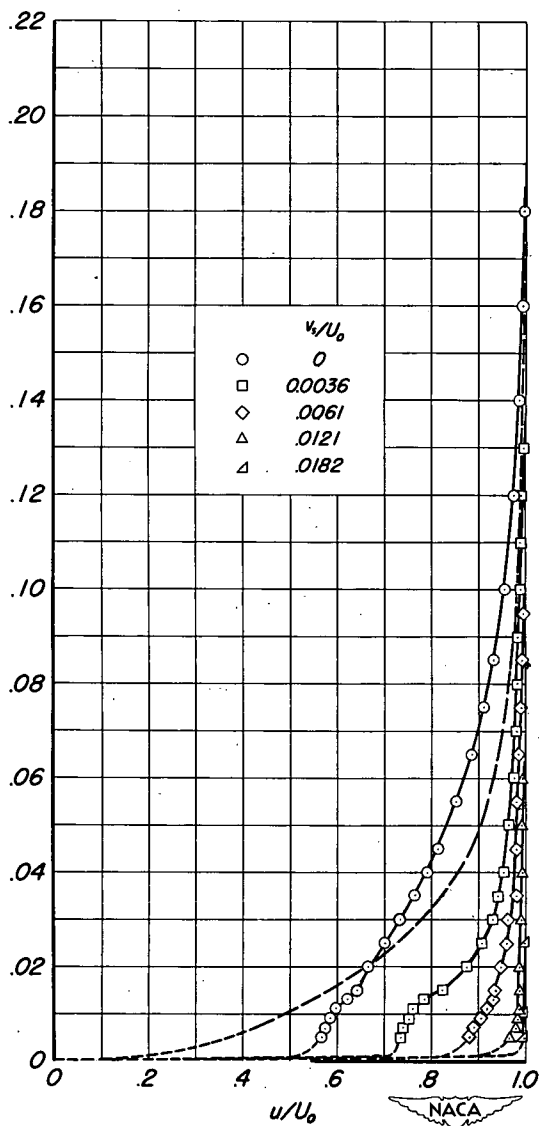
Figure 6 .—Continued.
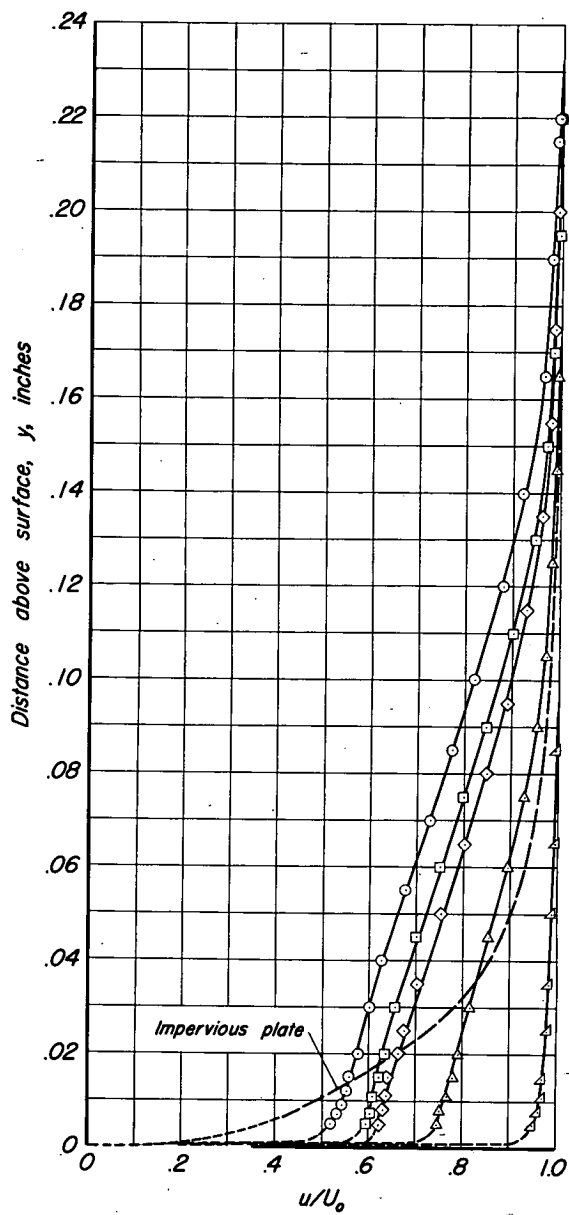
(e) Sample 5, (electroplated mesh, 40 count).
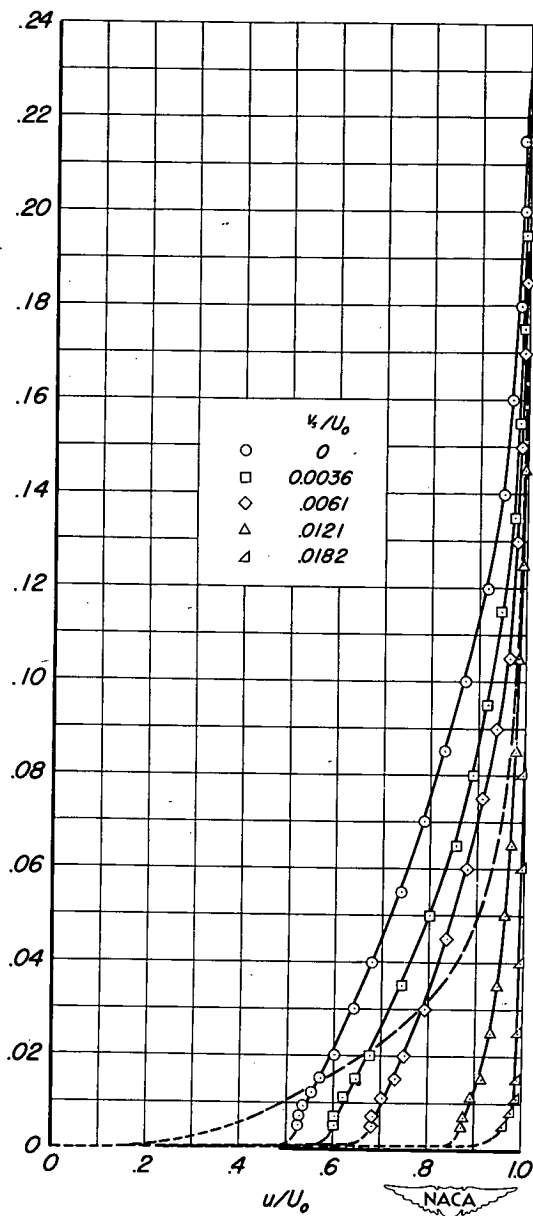
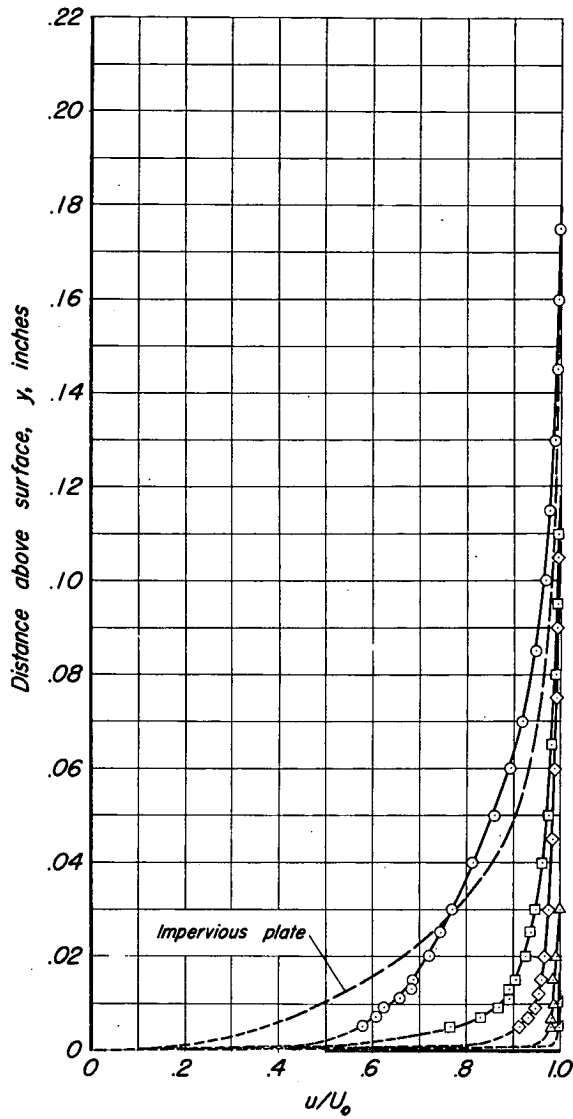(f) Sample 6, (electroplated mesh, 65 count).

Figure 6 .— Continued .
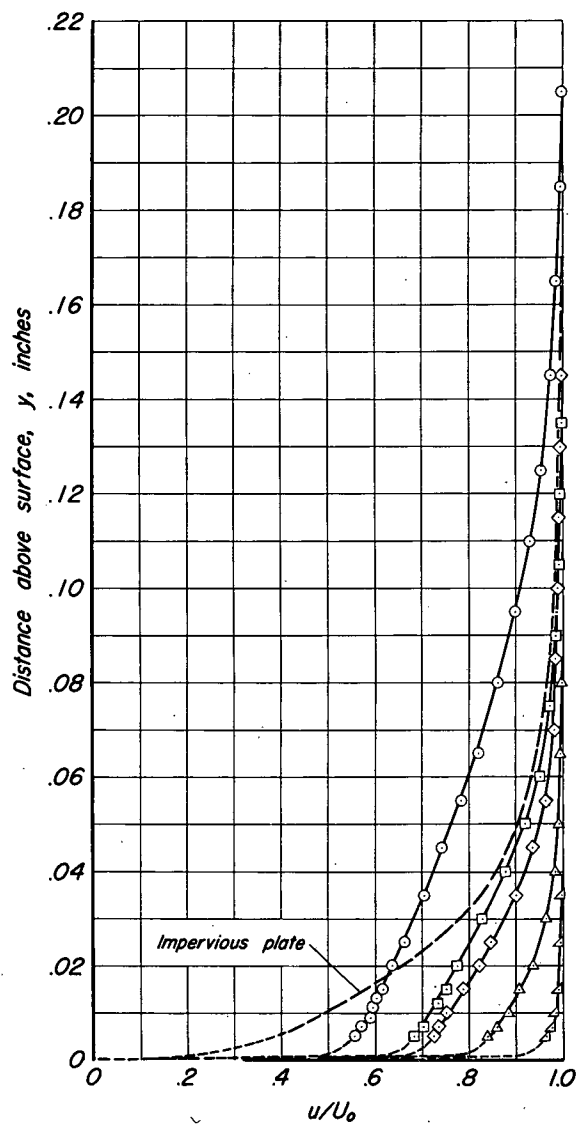
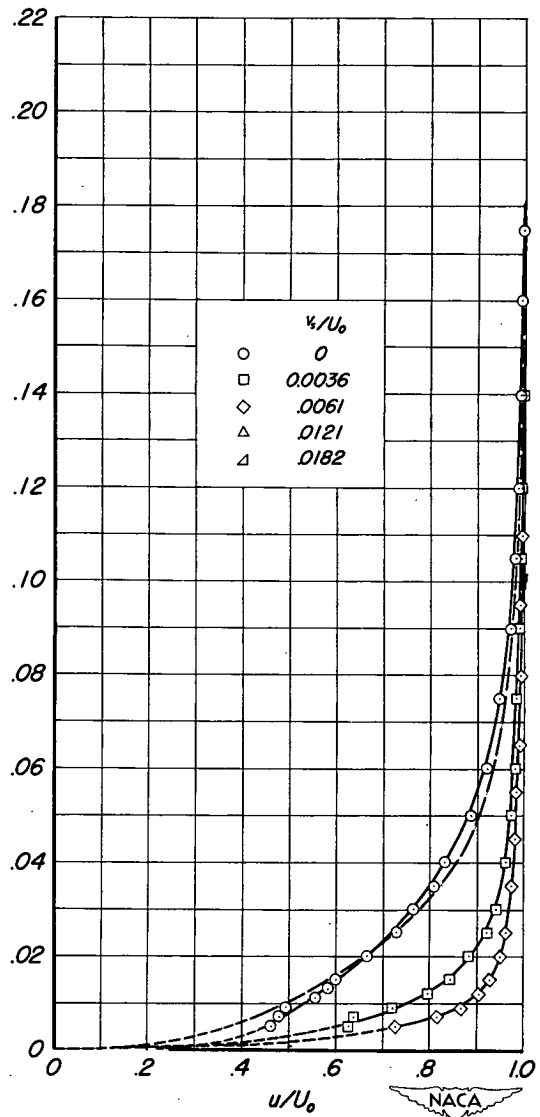(g) Sample 7, (sintered bronze).

(h) Sample 8, (sintered bronze).

Figure 6 .- Conti,

(i) Sample 9, (sintered bronze).

(j) Sample 10, (sintered bronze).
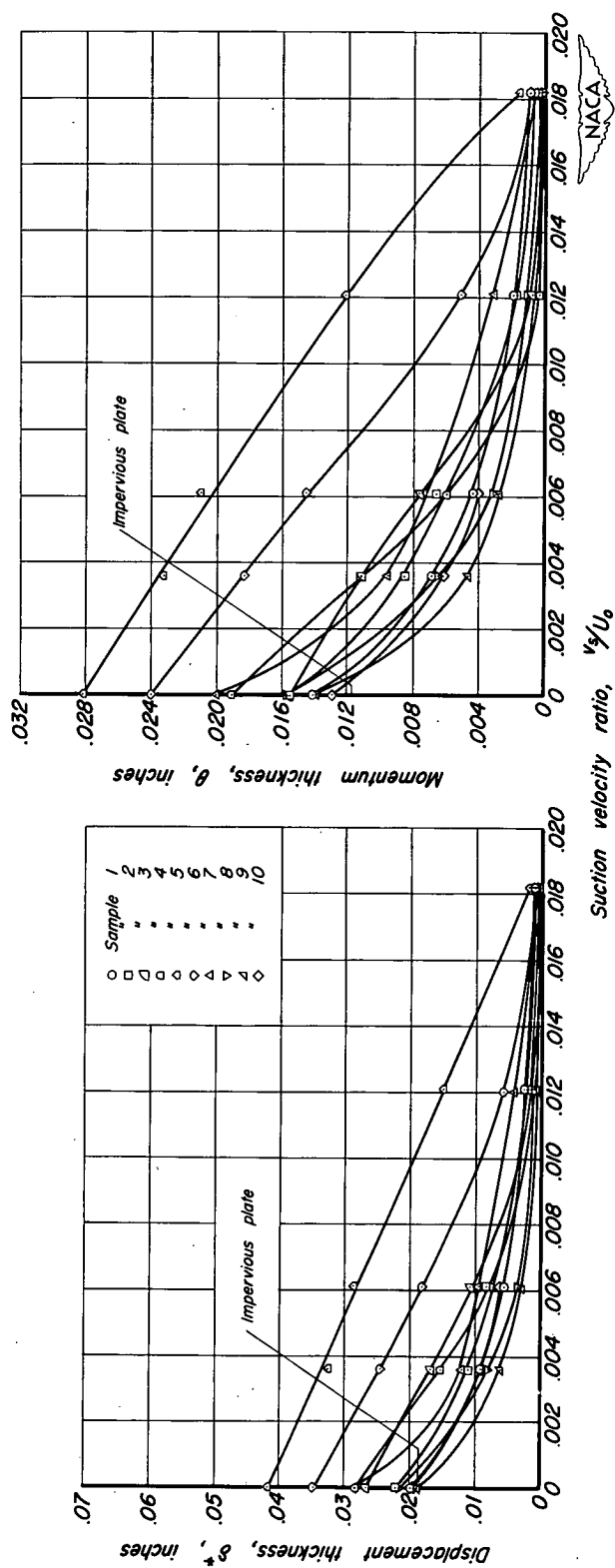
Figure 6 .- Concluded.

Figure 7 .- Variation of boundary-layer displacement thickness and momentum thickness with suction velocity ratio.